URSI GASS 2021, Rome, Italy, 28 August - 4 September 2021

Numerically Error-Controlled Computation of Gaussian-Beam Propagating Plane-Wave Fast Multipole Translation Operators

Thomas F. Eibert
Chair of High-Frequency Engineering
Department of Electrical and Computer Engineering
Technical University of Munich
80290 Munich, Germany

Abstract

The Gaussian beam concept allows to produce well focused propagating plane-wave fast multipole translation operators, where many of the plane-wave samples with small magnitudes can be dropped during the computation of the fast multipole spectral integrals over the Ewald sphere. However, the parameterization of the Gaussian beam operators and of the related numerical evaluation procedure is not easy. In order to overcome the related issues, a fully numerical procedure for the optimization of the Gaussian-beam parameters with appropriate error control is presented. This procedure is numerically very efficient and can be utilized in the pre-computation of fast multipole translation operators within fast multipole or multilevel fast multipole solutions of integral equations. The versatility and accuracy of this approach is demonstrated within a multilevel fast multipole accelerated inverse source-solver, which can efficiently handle large scale source distributions.

1 Introduction

The multilevel fast multipole method (MLFMM) has been the most powerful and flexible fast integral solver for many years [1]. It is routinely utilized for the solution of integral equations in the fields of radiation and scattering problems, more recently also for inverse-source problems [2, 3]. The key of the MLFMM is a factorized diagonal representation of the pertinent radiation operator in form of propagating planes waves, which requires the evaluation of a spectral integral over the Ewald sphere in k-space, involving source and receive k-space representations together with corresponding translation operators (TLOPs) [1]. The handling of all the plane-wave samples on the Ewald sphere during the evaluation of the spectral integral is responsible for the computational workload of the MLFMM and it can, therefore, be of advantage to look for improved formulations, which can produce accurate results with a reduced number of plane-wave samples. For large translation distances, the standard FMM TLOPs become more and more directive and eventually only one plane-wave smaple is required for the evaluation of the k-space integral [4]. Such a far-field method is, however, not very efficient in general and further improvements have been achieved by working with windowed translation operators, which are able to produce better focused TLOPs for shorter translation distances [5]. TLOPs with improved focusing in k-space can be achieved by the concept of Gaussian beams (GBs) [6], which have in particular been proven powerful for the solution of inverse-source problems [7, 8].

In this paper, some important properties of Gaussian-beam (GB) based FMM TLOPs are highlighted and a fully numerical approach for the error-controlled determination of its parameters is discussed.

2 The Fast Multipole Plane-Wave Expansion

The FMM formulation with propagating plane waves is commonly derived from the standard plane-wave Gegenbauer formula [1]

$$\frac{\mathrm{e}^{-jk|\mathbf{X}+\mathbf{d}|}}{|\mathbf{X}+\mathbf{d}|} = \lim_{L^S\to\infty} \oint\!\!\!\oint \mathrm{e}^{-j\mathbf{k}\cdot\mathbf{d}}\, T_L^S(\hat{k}\cdot\hat{X}, X)\,\mathrm{d}^2\hat{k}, \tag{1}$$

which is convergent for $X = |\mathbf{X}| > d = |\mathbf{d}|$. The involved standard plane-wave FMM TLOP T_L^S can be expressed as a series expansion with orthogonal Legendre polynomials (LPs) in the form of

$$T_L^S(\hat{k}\cdot\hat{X}, X) = \sum_{l=0}^{L^S} c_l^S(X)\,\mathrm{P}_l(\hat{k}\cdot\hat{X}) \tag{2}$$

where the expansion coefficients are

$$c_l^S(X) = \frac{-jk}{4\pi}(-j)^l(2l+1)\mathrm{h}_l^{(2)}(kX) \tag{3}$$

and where $\hat{k}$ and $\hat{X}$ are the unit vectors in the direction of $\mathbf{k}$ and $\mathbf{X}$, respectively. With the decomposition

$$\mathbf{r}-\mathbf{r}' = \underbrace{(\mathbf{r}_m-\mathbf{r}'_s)}_{\mathbf{X}} + \underbrace{\mathbf{r}-\mathbf{r}_m-(\mathbf{r}'-\mathbf{r}'_s)}_{\mathbf{d}}, \tag{4}$$

of the vector difference between an observation location $\mathbf{r}$ and a source location $\mathbf{r}'$ together with a fixed plane-wave source expansion center $\mathbf{r}_s'$ and a fixed observation expansion center, e.g., $\mathbf{r}_m$, the scalar Green's function of the Helmholtz equation and the related dyadic Green's functions of radiation, scattering, and inverse-source problems [1] can be factorized via (1) and a diagonal representation of radiation integrals as basis of a fast computational evaluation for many source and observation locations can be derived [3, 8].

For numerical evaluation, the maximum series order L^S in (2) is limited to a finite value, which is often selected by the approximate rule [1]

$$L^S = kd/2 + 1.8 d_0^{2/3} (kd/2)^{1/3}, \tag{5}$$

where 10^{-d_0} is the relative error for the maximum applicable d.

3 Gaussian-Beam Translation Operators

With an imaginary spatial displacement Δ according to

$$\mathbf{X} + \mathbf{d} = \mathbf{X} - j\Delta\hat{X} + \mathbf{d} + j\Delta\hat{X}, \tag{6}$$

the standard plane-wave Gegenbauer formula in (1) can be continued into complex space, where a modified GB TLOP is obtained in the form of [6]

$$T_L^G(\hat{k}\cdot\hat{X}, X, \Delta) = \mathrm{e}^{k\Delta(\hat{k}\cdot\hat{X})} \sum_{l=0}^{L^G} c_l^S(X - j\Delta)\mathrm{P}_l(\hat{k}\cdot\hat{X}). \tag{7}$$

The focusing properties of this TLOP can be influenced by appropriately choosing Δ. However, care should be exercised, since the achievable accuracy of the formulation depends strongly on Δ. A lager summation limit L^G allows to work with larger values of Δ.

Since the exponential factor $\mathrm{e}^{k\Delta(\hat{k}\cdot\hat{X})}$ in (7) modifies the functional dependence with respect to $\hat{k}\cdot\hat{X}$ as given by the actual LP-series expansion, we perform a re-expansion according to

$$\hat{T}_L^G(\hat{k}\cdot\hat{X}, X, \Delta) = \sum_{l=0}^{L_o^G} c_l^G(X, \Delta)\mathrm{P}_l(\hat{k}\cdot\hat{X}) \tag{8}$$

with

$$c_l^G(X, \Delta) = \int_{-1}^{+1} T_L^G(x, X, \Delta)\mathrm{P}_l(x)\,\mathrm{d}x. \tag{9}$$

The expansion coefficients c_l^G can be directly compared to the expansion coefficient c_l^S of the standard TLOP in (3). In (8), $L_o^G \geq L^G$ should be chosen to take care of the fact that the exponential factor with $\Delta > 0$ leads to a larger spectral extent of the TLOP. In a numerical FMM or MLFMM implementation, sub-sampling of the GB TLOP may, however, be recommended, as long as the introduced aliasing errors are kept under control.

In Fig. 1, standard and GB TLOPs are illustrated dependent on ϑ (for translation in z-direction), where the LP series truncation limits L^S and L^G and the imaginary shift Δ for the GB TLOPs are the same for both cases (1 and 2), but the translation distances are different. For the larger translation distance, the standard TLOP is considerably more focused than for the shorter distance. However, the TLOP magnitudes for larger ϑ (sidelobes) are not falling below -60 dB and truncation of the spectral integral is, therefore, not possible with standard TLOPs, if an error level of -70 dB or better -80 dB is required. The magnitudes of the GB TLOPs show both a very steep decay for increasing ϑ and fall below -80 dB at around $\vartheta = 20^o$. Figure 2 depicts the LP series coefficient magnitudes corresponding to the TLOPs in Fig. 1, and Fig. 3 the corresponding phases. In particular together with the relative errors of the GB LP expansion coefficients with respect to the coefficients of the standard TLOPs in Fig. 4, it becomes clear that the GB TLOPs maintain the lower order coefficients, but modify the coefficients with higher orders in order to achieve the focusing. Since accurate radiation operator evaluations are only possible for source and receive spectra, which do not contain such higher-order terms, GB TLOPs should only be utilized for small enough source/receive groups, which do not excite such higher-order terms, or, alternatively, we

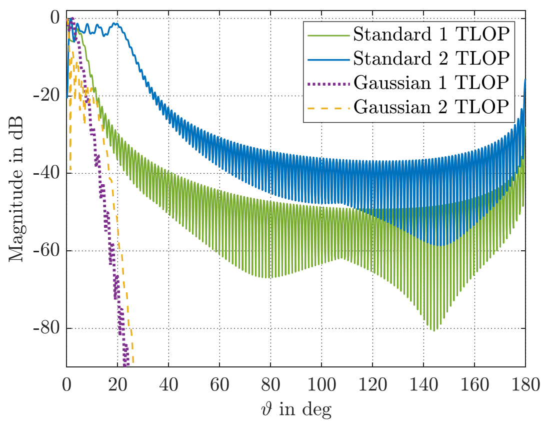

Figure 1. Illustration of TLOPs for translation distances $X_1 = 150\lambda$ (1) and $X_2 = 50\lambda$, $L^S = 138$, GB TLOPs with $\Delta = 12\lambda$, $L^G = 95$ in (7). Sub-sampled TLOPs would look equal except for the missing samples.

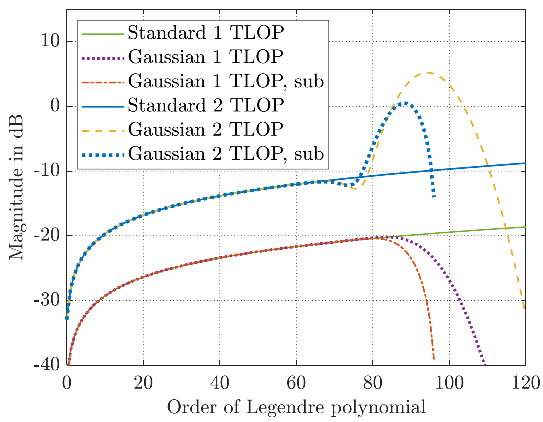

Figure 2. LP expansion coefficient magnitudes for the TLOPs in Fig. 1. "sub" indicates sub-sampled TLOPs generated on a sampling grid appropriate for LP indices up to 95.

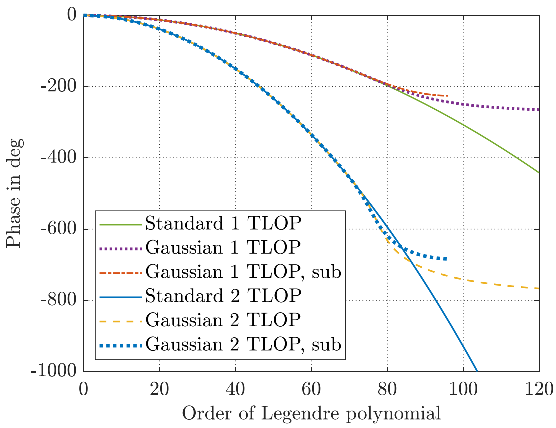

Figure 3. LP expansion coefficient phases for the TLOPs in Fig. 1. "sub" indicates sub-sampled TLOPs generated on a sampling grid appropriate for LP indices up to 95.

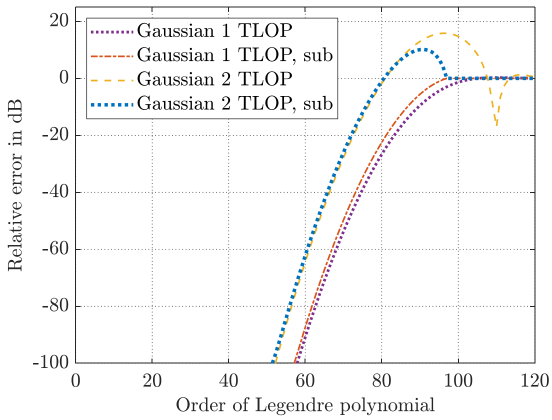

Figure 4. Relative errors of the GB LP expansion coefficients with respect to the standard TLOP coefficients for the TLOPs in Fig. 1. "sub" indicates sub-sampled TLOPs generated on a sampling grid appropriate for LP indices up to 95.

can say that the GB TLOPs should work with a somewhat larger order L^G and corresponding to this, with some finer sampling of the spectral integrals. A certain degree of sub-sampling of the higher-order terms, can in general be afforded and is recommended, if the introduced aliasing error is kept under control, as also illustrated in the figures.

4 Error-Controlled GB TLOP Computation

The standard FMM TLOP in (2) is fully determined, once the number of LP-terms L^S has been selected for the required accuracy. The corresponding quadratue and sampling rules for the spectral integral computation are then easy to set [1]. For GB TLOPs, it is recommended to work with a larger number of LP series terms in order to achieve well focused TLOPs for a given accuracy level. Therefore, we consider GB TLOPs for a sampling grid appropriate for L_o^G in (8), i.e., with $L_o^G + 1$ ϑ-samples and $2L_o^G$ φ-samples, and with

$$L_o^G = f^{OS} L^S , \qquad (10)$$

where f^{OS} is an oversampling factor, which may advantageously be chosen in the range $f^{OS} = 1.1 \ldots 1.2$.
In order to determine the GB TLOP parameters L^G and Δ in (7), we consider the specific relation

$$\frac{\mathrm{e}^{-jk|X\hat{z}+d\,\hat{z}|}}{|X\hat{z}+d\,\hat{z}|} = \oiint T_L(\hat{k}\cdot\hat{z}, X)\mathrm{e}^{-j\mathbf{k}\cdot d\,\hat{z}}\,\mathrm{d}^2\hat{k} \qquad (11)$$

obtained from (1) by setting $\mathbf{X} = X\hat{z}$, i.e., translation along the z-axis, and $\mathbf{d} = d\,\hat{z}$, i.e., source and observation locations on the z-axis. Thee "=" has been kept in the equation, despite the lim over L is not considered anymore. The expression left of the "=" can be directly computed as a reference value for the considered translation process. The φ-integration of the spectral integral on the right-hand side of the equation gives just the factor 2π and with consideration of (8), (11) results in

$$\frac{\mathrm{e}^{-jk|X+d|}}{|X+d|} = 2\pi \sum_{l=0}^{L_o^G} c_l^G(X,\Delta) \int_{x=-1}^{+1} \mathrm{e}^{-jkxd}\,\mathrm{P}_l(x)\mathrm{d}x + \varepsilon , \qquad (12)$$

which can easily be evaluated by numerical quadrature. ε is here the error due to the employed FMM procedure. It comprises the errors due to the LP-series truncation and the error due to the numerical quadrature. Choosing d as the largest relevant value within the FMM procedure gives the worst-case error, where the given consideration is, however, only valid for the case of source and observation locations on the z-axis. An important advantage of this simplified representation is that it only requires a one-dimensional integration, which can efficiently be performed numerically, where an extension of the approach to arbitrarily located source and observation locations is also possible.
Based on the error ε in (12), numerically error-controlled optimization of the the GB TLOP parameters, L^G and Δ in (7) can be performed, which is efficient enough for the computation of all the required GB TLOPs in an FMM or MLFMM solution of integral equations of large-scale radiation, scattering, or inverse-source problems. A more general error-controlled computation scheme for GB TLOPs is found in [9].

5 Numerical Results

For a numerical inverse-source solution based on an MLFMM approach [3, 10], we consider a virtual radiating aperture as illustrated in Fig. 5 for a frequency of 40 GHz. The tapered linearly polarized aperture source distribution is modeled by Hertzian dipoles on a regular grid, which were used to compute the near-field (NF) samples on the scan plane (34 969 sample locations on a regular square grid with two orthogonal electric field components observed at each location) and the reference far fields (FFs). Inverse-source solutions with distributed spherical harmonics expansions [3] were computed in order to obtain the FF pattern of the aperture, where two orthogonal pattern cuts are illustrated in Fig. 6 and Fig. 7. The MLFMM accuracy was set to −76 dB and solutions with standard TLOPs as well as with error-controlled GB TLOPs as described in this paper

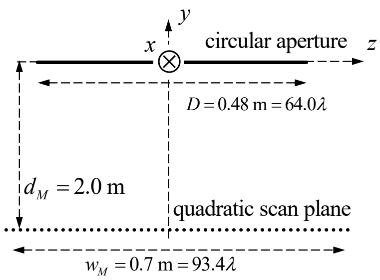

Figure 5. Geometry of virtual radiation aperture with obersvation scan plane.

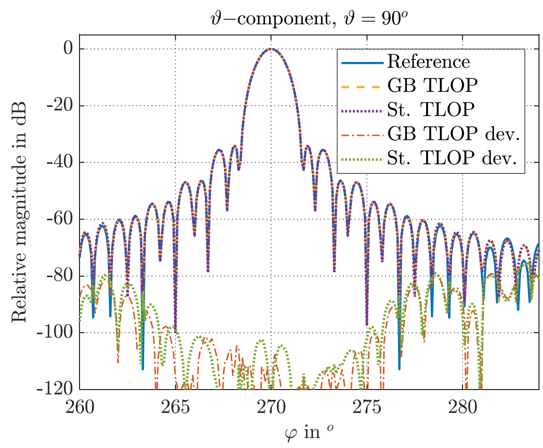

Figure 6. Co-polar FF pattern cut of radiation aperture according to Fig. 5. Inverse-source results with standard (St.) and GB TLOPs are compared to reference data.

were computed. The FF error level in the main beam (linear magnitude difference over pattern maximum) goes well below −100 dB with both TLOPs, where the utilization of the GB TLOPs leads for this arrangement to a speed-up by a factor of more than 10 and a memory reduction (RAM) of more than a factor of 3.

6 Conclusion

The focusing properties of Gaussian-beam propagating plane-wave fast multipole translation operators were investigated and a fully error-controlled numerical scheme for the efficient determination of the corresponding parameters was discussed. Numerical results with a multilevel fast multipole method accelerated inverse-source solver demonstrated the accuracy and the efficiency of the approach.

References

[1] W. C. Chew, J.-M. Jin, E. Michielssen, and J. Song, *Fast and Efficient Algorithms in Computational Electromagnetics*. Boston: Artech House, 2001.

[2] T. F. Eibert and C. H. Schmidt, "Multilevel fast multipole accelerated inverse equivalent current method employing Rao-Wilton-Glisson discretization of electric and magnetic surface currents," *IEEE Transac-

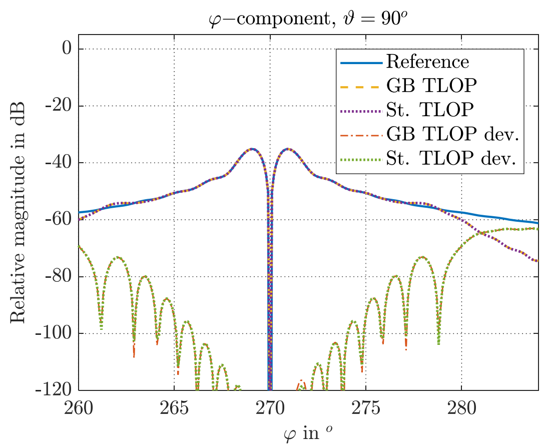

Figure 7. Cross-polar FF pattern cut of radiation aperture according to Fig. 5. Inverse-source results with standard (St.) and GB TLOPs are compared to reference data.

tions on Antennas and Propagation, vol. 57, pp. 1178–1185, 2009.

[3] T. F. Eibert, E. Kilic, C. Lopez, R. A. Mauermayer, O. Neitz, and G. Schnattinger, "Electromagnetic field transformations for measurements and simulations (Invited Paper)," *Progress In Electromagnetics Research*, vol. 151, pp. 127–150, 2015.

[4] W. C. Chew, T. J. Cui, and J. M. Song, "A FAFFA-MLFMA algorithm for electromagnetic scattering," *IEEE Transactions on Antennas and Propagation*, vol. 50, pp. 1641–1649, 2002.

[5] T.-J. Cui, W. C. Chew, and J. Song, "Efficient MLFMA, RPFMA, and FAFFA algorithms for EM scattering by very large structures," *IEEE Transactions on Antennas and Propagation*, vol. 52, pp. 759–770, 2004.

[6] T. B. Hansen, "Translation operator based on Gaussian beams for the fast multipole method in three dimensions," *Wave Motion*, vol. 50, pp. 940–954, 2013.

[7] T. B. Hansen and O. Borries, "Gaussian translation operator in a multilevel scheme," *Radio Science*, vol. 50, pp. 754–763, 2015.

[8] T. F. Eibert, D. Vojvodic, and T. B. Hansen, "Fast inverse equivalent source solutions with directive sources," *IEEE Transactions on Antennas and Propagation*, vol. 64, pp. 4713–4724, Nov. 2016.

[9] T. F. Eibert and T. B. Hansen, "Propagating plane-wave fast multipole translation operators revisited — standard, windowed, Gaussian beam," *IEEE Transactions on Antennas and Propagation*, vol. 69, 2021, accepted for publication.

[10] J. Kornprobst, R. A. Mauermayer, O. Neitz, J. Knapp, and T. F. Eibert, "On the solution of inverse equivalent surface-source problems," *Progress In Electromagnetics Research*, vol. 165, pp. 47–65, 2019.